

## UT-VIV/AM-AIA

### Task title: TECHNOLOGIES FOR VACUUM AND TEMPERATURE CONDITIONS FOR REMOTE HANDLING SYSTEMS ARTICULATED INSPECTION ARM (AIA)

#### INTRODUCTION

This project takes place in the Underlying Technologies (UT) in Remote Handling (RH) activities. The aim of the R&D program is to demonstrate the feasibility of close inspection of the Divertor cassettes and the Vacuum Vessel first wall of ITER. We assumed that a long reach and limited payload carrier penetrates the first wall using the 6 penetrations evenly distributed around the machine and foreseen for the In-Vessel Viewing System (IVVS).

The need, to access closer than the IVVS to the Vacuum Vessel first wall and the Divertor cassettes, had been identified. This is required when considering inspection with other processes as camera or leak detection.

The work performed under the EFDA-CSU Workprogramme includes the design, manufacture and testing of an articulated device demonstrator called Articulated Inspection Arm (AIA).

The AIA has to fulfil the following specifications:

- Elevation: + - 45° range,
- Rotation: +- 90° range,
- Robot total length: 7.4 meters,
- Admissible payload: 10 Kg,
- Temperature: 200°C during baking – 120°C under working,
- Pressure:  $9.7 \cdot 10^{-6}$  Pa – Ultra high vacuum.

The manufacture and procurement activities of the AIA robot are performed within the TW5-TVR-AIA Task.

#### 2006 ACTIVITIES

##### PROTOTYPE MODULE ACTIVITIES SUMMARY

The past year was dedicated to the segment cycling test campaign in real operating conditions in CEA-Cadarache facilities to validate all the robot components. The successful results enable to start the whole robot manufacture and procurement.

Succeeding maintenance and expertise operations, a new test campaign in Tore Supra facility ME60 is currently carried on to fully qualify the robot under vacuum and temperature conditions.

##### TEMPERATURE AND ULTRA HIGH VACUUM TESTS IN ME60

Following the test campaign at air pressure and ambient temperature in CEA-Fontenay aux Roses facilities in 2005, and while the new elevation roller screw manufacture was

under progress, the prototype module was submitted to a real functioning conditions test campaign with 80 kg load in ME60 CEA-Cadarache facilities in July 2006.

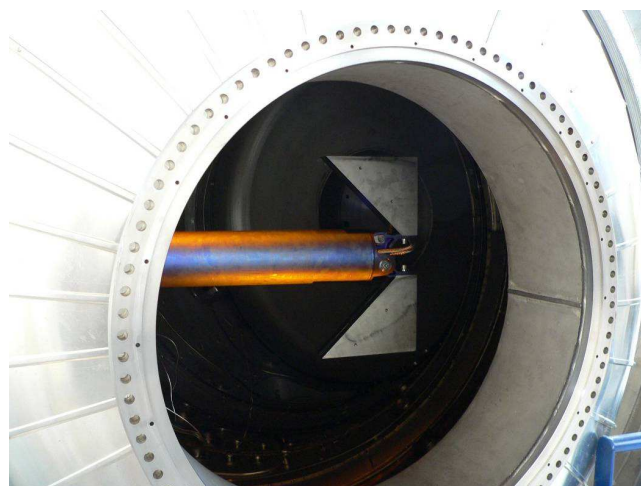


Figure 1: Prototype module test campaign in ME60 facility July 2006

Cycle is composed of rotation combinations:

Table 1: A representative cycle during the test campaign in CEA-Cadarache

Points	Elevation (°)	Rotation (°)	Waiting time (s)
1	0	17	60
2	0	-9	60
3	0	10	60
4	0	30	60
5	0	-5	60
6	0	0	60

After about 200 cycles on the rotation axis, the test was interrupted. A maintenance phase was programmed to replace some components and integrate upgrades on the elevation jack.

##### 80°C TEMPERATURE AND AIR PRESSURE TEST CAMPAIGN

Following the maintenance phase, the prototype was still operational and was mounted on its pillar with the heating device and 80 kg at its extremity.

The tests campaign was carried on at 80°C temperature and ambient conditions.

Table 2: A representative test during the ambient temperature test campaign

Points	Elevation (°)	Rotation (°)	Waiting time (s)
1	0	17	60
2	8.5	-9	60
3	6	12	60
4	0	30	60
5	-8.5	-6	60
6	0	0	60

500 cycles were performed on the elevation axis. The test campaign was stopped because it was noticed a slow augmentation of the elevation motor consumption (reaching 2.2 Amps).

An expertise phase was performed in CEA-Fontenay aux Roses in order to explain the reason of this augmentation. The conclusions pointed out a lack of grease in the roller screw functioning zone, due to the intrinsic helicoidal movement between the screw and the nut.

This problem can be solved easily by an elevation motor consumption surveillance and a preventive lubrication when the robot reaches 500 cycles, which is half of the robot life time, estimated to 1000 cycles. Upgrades were integrated on the jack to make easier this maintenance phase.

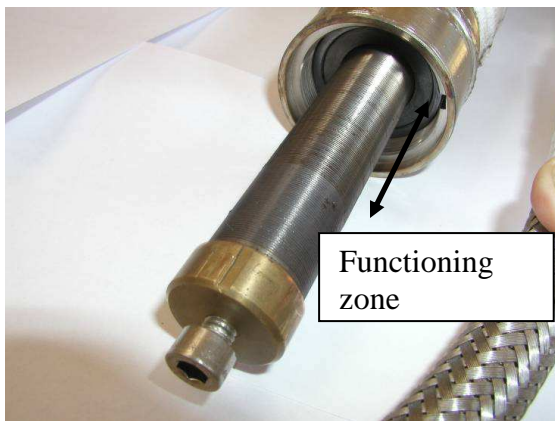


Figure 3: Lack of grease in the functioning zone of the roller screw

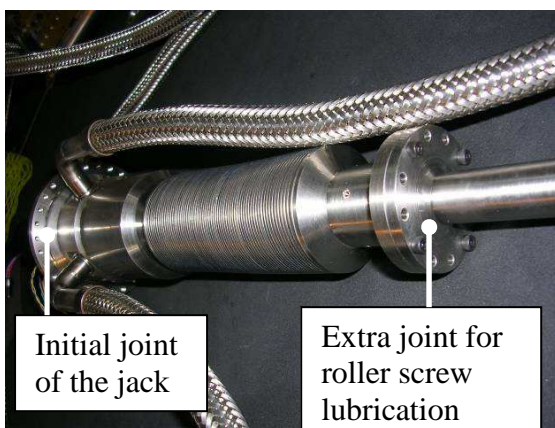


Figure 4: Integration of a joint in the elevation jack S4-S5

## MOTOR TESTS

During the several test campaigns performed in real temperature conditions in CEA-Cadarache, we noticed several problems on the motors used in the AIA robot. Because the efficiency of these motors doesn't cope with our requirements, the CEA-Fontenay aux Roses decided to pursue advanced tests on another motor brand. The manufacturer specifies a maximum temperature range up to 125°C for the motor and up to 155°C for the rotor itself.

The motors were submitted to several baking tests followed by 120°C functioning phases to verify the motor well behaviour.

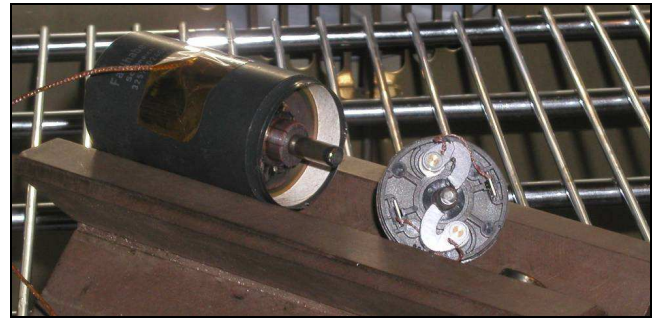


Figure 5: Motor observation after a 180°C baking test

Considering the replacement of the existent bearings by high temperature lubricated bearings, the motors were tested in CEA-Fontenay aux Roses to validate on a test bench the efficiency of these upgraded motors.



Figure 6: Motor bearings replacement

The 200°C baking tests and 120°C functioning tests validate the upgraded gear motor efficiency for AIA application. Therefore, they are retained to be integrated in the AIA robot. This solution qualification is now under progress on the prototype module in the ME60 CEA-Cadarache facilities. Two of these motors were integrated on the module to validate the solution in real Tokamak conditions. The first results seem to confirm the solution efficiency.

## INTERSEGMENT UMBILICALS

The objective of this test is to demonstrate the feasibility of connecting 2 AIA segments with external umbilicals. The qualification test is performed on the segment 4-5 articulation which is the most complex articulation of the robot. The difficulty of this design is that the umbilical must be stressed around only one degree of freedom at a time.



*Figure 7: The new design for 4-5 articulation*

This design validates the solution to connect 2 AIA segments by an exterior umbilical. The cycling tests cope with the AIA requirements because the umbilical support far more than the AIA service life. It reaches 9000 cycles (corresponding to a trajectory between  $-90^\circ$  and  $90^\circ$ ) which is much higher than the AIA robot operating duration for the 4-5 articulation.

## CONCLUSIONS

---

Demonstration of the AIA intervention feasibility in real temperature and vacuum Tokamak environment is foreseen for 2007 on Tore Supra.

The results on this multipurpose robotic device give new perspectives on maintenance and operating activities for a reactor like ITER and aim to enhance operator perception of in-vessel situation.

## REPORTS AND PUBLICATIONS

---

CEA/DTSI/SRI/LRM/ 07RT.008-Issue 0 Prototype module, vacuum and temperature technologies test report.  
Delphine KELLER

## TASK LEADER

---

Jean Pierre FRICONNEAU

DRT/DTSI/SRSI  
CEA-Fontenay aux Roses  
Boîte Postale 6  
F-92265 Fontenay aux Roses Cedex

Tel. : 33 1 46 54 89 66

Fax : 33 1 46 54 75 80

e-mail : jean.pierre.friconneau@cea.fr

## Task Title: RADIATION EFFECTS ON ELECTRONIC TECHNOLOGIES AND COMPONENTS

### INTRODUCTION

The significant acceleration of the CMOS submicronic technology roadmap now implies a very short time for the design and manufacturing of components and complex systems. Massive parallel computers as well as low power embedded applications (wireless networks...) are designed to realise services always in expansion while the number of chips significantly decreases. The great complexity of the die itself, but also the small space allocated to the chip on the end-user board (most recent components are connected with balls on the package back side) require to modify the usual approach to understand the behaviour of such technologies under severe environments.

Studies on STMicroelectronics HCMOS7 (250nm) were driven on both logic components and functions (JTAG state machine used to control the die). The  $\gamma$  rays radiation tolerance was evaluated to more than 1MGy which confirms the intrinsically expected hardening.

Year 2006 was mainly focused on how to realise a test bench representative of both recent STMicroelectronics technology (HCMOS9 130nm) and ongoing concrete case applications.

### 2006 ACTIVITIES

#### HCMOS9 technology

This technology is available on market since the end of 2001. The main useful characteristics were:

- Low power supply of 1.2V with possible extension to 2.5V and 3.3V
- Three transistor families (very low and low leakage, high speed)
- Threshold voltage (570/500/380 mV) and Isat (high level 410/535/680 $\mu$ A/ $\mu$ m; low level 170/240/320 $\mu$ A/ $\mu$ m)

As for previous technologies, non basic components were provided to realise test vectors. The only way was to define functions to be integrated in an ASIC and realise it through Multi-Project Chips developments tools.

#### Test vector

Regarding partial significant results already published [1], [2] concerning the Total Integrated Dose tolerance evaluation of HCMOS9 basic components initially irradiated by CERN teams to 1MGy, it appears that the threshold voltage becomes more stable while the leakage current decreases by an order 2-3 of magnitude for the oldest technologies.

Even if those results did not reach TID supported by future in-vessel maintenance engines, we decided to focus our work on more realistic embedded developments.

The choice we made was led by the work developed around a PhD thesis concerning the control unit for embedded multi processors architecture [3].

An ASIC was realised for the implementation of this control unit using industrial methods and tools starting from the model design up to the lay out. As seen on figure 1, each step of the design was completed by a model description in order to be simulated. This simulation gave us a significant verification of the main functions in term of connexions, timing ...

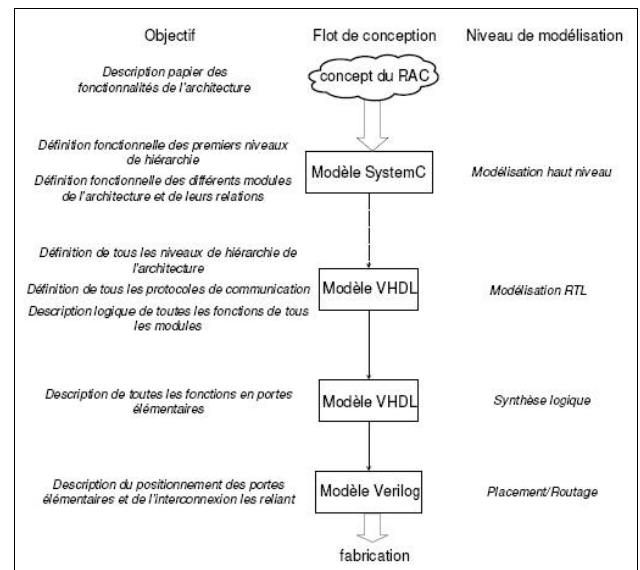


Figure 1: Method used to define and realise the ASIC

It was clear that the method developed here was not fully necessary to know the behaviour under severe environment; nevertheless, the description of some of the functions, their implementation with very simple logic circuits and finally the lay out (see figure 2) and the pins configuration let us use them as appreciable test vectors.

The module was sent to fab at the end of 2005.

Unfortunately, the verification test done when the ASIC was received in first trimester 2006 gave a great number of non functional states. As explained by the designers, it needed long term operations to recover some basic functions that may not be available before a few months.

The characterization under severe environments, temperature and radiation is planned for 2007.

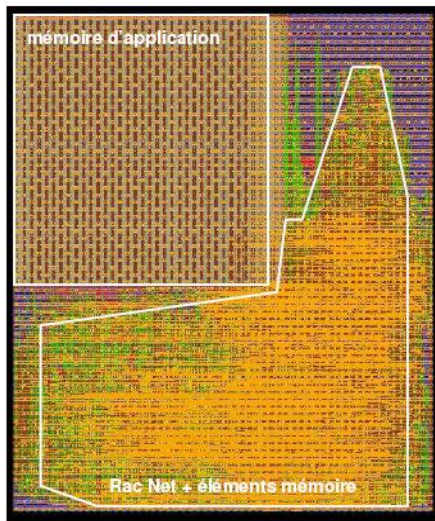


Figure 2: Lay out of the control module

**JTAG investigations**

As already reported on [1], evaluation of HCMOS7 was done with a JTAG module associated with simpler invertors.

The main interest of such modules was to create a shift register able to push binary input values and pop binary output to specific test points internally extended to part of the full function of the chip. This mechanism allows the individual test of functions or electronic systems and the observation of internal data links. Then, it would be possible to find failed functions or erroneous link states (open or short circuits for example).

The two main aspects driven by the use of such tools concern the packaging which always limit or suppress the open eye control on test or functional pins, and secondly as presented on figure 3 the assertion of test vectors to validate the reliability or to find native or ageing erroneous states.

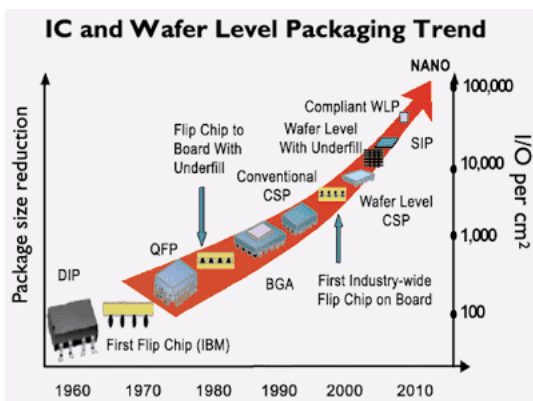


Figure 3: High scale integration during 50 years

The picture on figure 4 shows the “virtual” nails to see the present configuration of blue test boxes inputs, the red continuous dash IN to OUT binary data link used to carry or extract test data to or from the blue test boxes and grey shapes used to replace functions.

The share of JTAG integrated circuits has significantly increased since external control can now not be done using usual nails pads. Complex industrial packaged components, or IPs (such as FPGA, DSP, PLD but also proprietary ASIC) are equipped with internal JTAG modules.

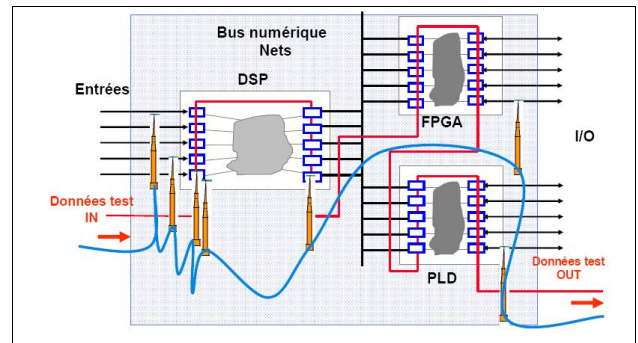


Figure 4: Example of JTAG applications on a multi core chip

On the other way, JTAG concept could be also applied to industrial usual components already available on the market by adding complementary JTAG registers to replace the blue boxes of figure 4.

As illustrated on figure 5, the blue shape holding a specific function could be encapsulated with input or output of JTAG registers in order to apply nominal or test conditions and catch nominal or test results through the JTAG red continuous line. In the same context, memories which never use JTAG control could be also inspected.

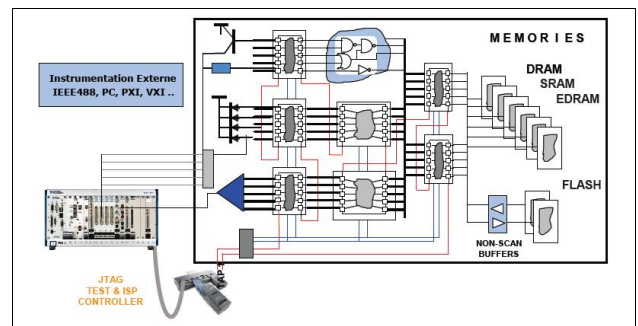


Figure 5: Cluster JTAG control

Based on these concepts, we decided to design dedicated clusters associated with JTAG registers and build test benches to create external dynamic state and drive JTAG elements.

Research of useful and common digital components for severe environments embedded applications led us to choose non volatile memories, in particular high density FRAM memory.

Concrete applications for civil nuclear purpose already use these memories with good results for low total dose levels [5] Smart complex applications, even in such environments, increase the need for large size memories.

The usual way to characterise memories under radiation was to consider them as peripheral of microcontrollers and access addresses or data fields through their input/output ports. In such cases, a specific test board was realised and specific protections were applied to avoid any controller failure under environmental effect.

Specific algorithms were developed to organise read and write accesses to memories bytes as pertinent as possible in order to detect failed states (blocked, non permanent write, etc).

The recent marketing of large size parallel FRAM (manufactured by RAMTRON) but also samples of

already available MRAM memories (manufactured by FREESCALE) seem an appreciable test vector.

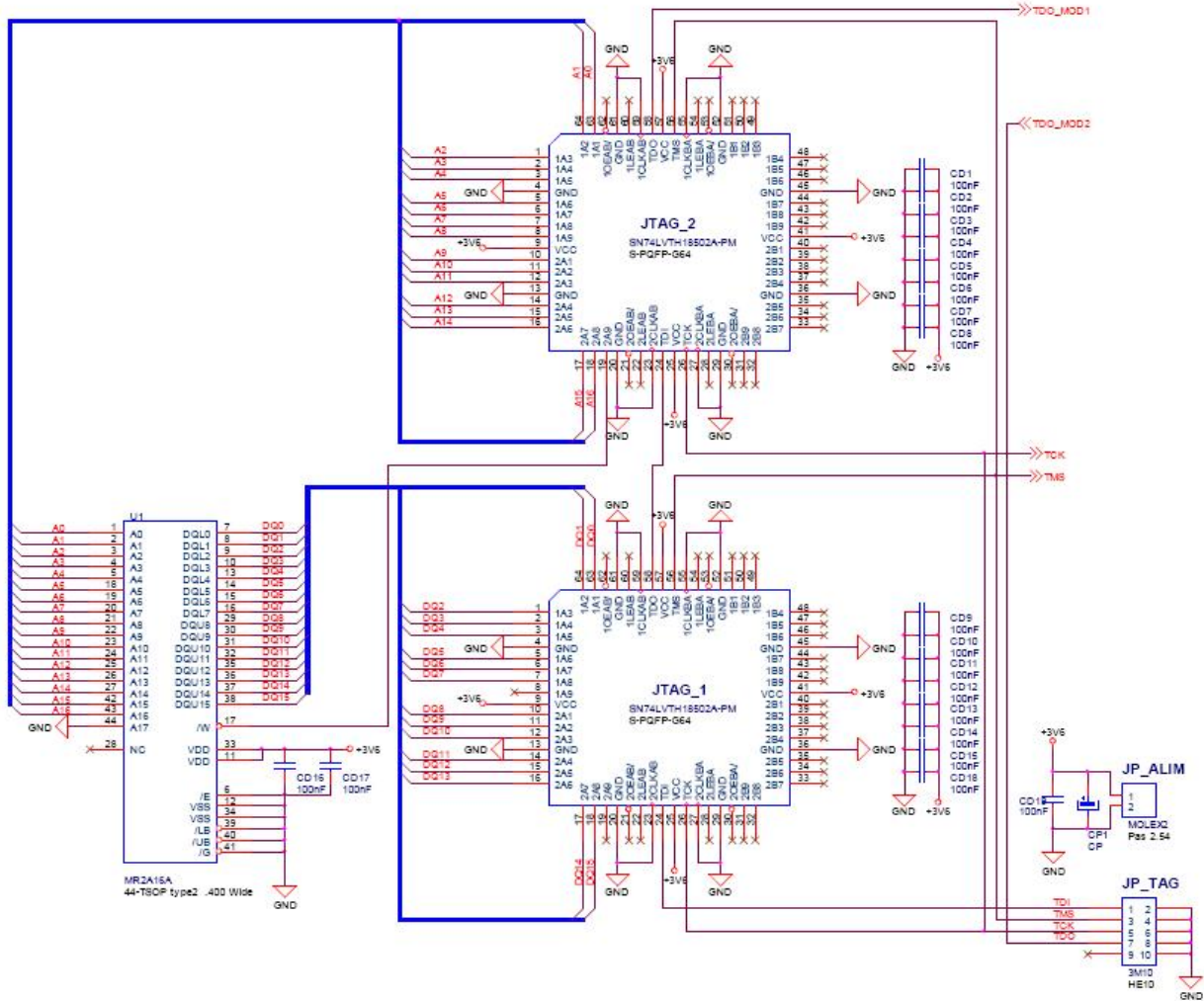


Figure 6: Test bench of MRAM memories using JTAG components

Firstly, their availability under severe environments will bring an immediate positive response for some autonomous embedded applications developed by our laboratory; secondly, they can be seen as large scale evaluation vectors under severe environments (temperature, total dose but also neutrons from different sources).

We decided to rebuild our old-fashioned memory test bed unable to manage new types of memories with JTAG test principles.

Taking into account the test organization presented in figure 5, we developed a test bench board for each of these memories using JTAG registers and link.

As shown on figure 6, the IN/OUT memory pins are accessible through JTAG registers (manufacturer Texas-Instrument).

The algorithms previously implemented on a microcontroller are executed through the JTAG link on an external PC control (see figure 7) and transferred into binary test vectors to be sent to or to be read from the JTAG registers. The schedule of these operations is performed conformably to the IEEE-1149 protocol.

By the end of the year 2006, the new experimental test bench is ongoing. Test boards are defined and started to be realised.

Instrumentation accessories like IEEE488 are mounted. JTAG elements are to be soon provided.

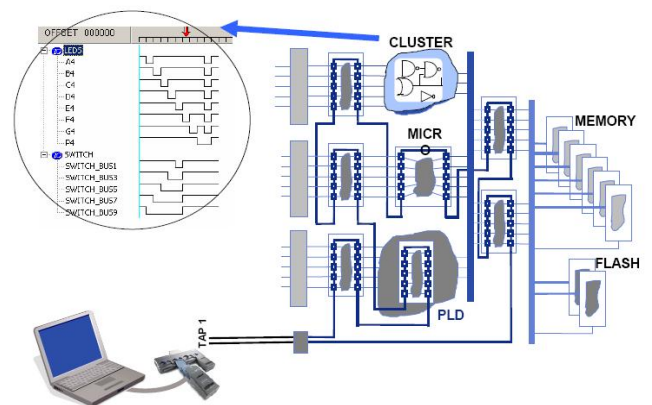


Figure 7: Floating ground and carrier current association

## CONCLUSIONS

---

The volontaire approach to use recent ASIC technology as vectors to evaluate severe environment tolerance was very difficult to assume and to lead to a successful operation.

This relative setback forced us to open our strategy on the behaviour of “on the shelf” recent or emerging components inserted into severe environment. The JTAG standard, commonly used to test (but also to on-line diagnose) large scale integration commercial or proprietary ASICs has to be investigated for our developments.

Year 2006 was dedicated to design and build the test bench.

Year 2007 will normally lead to use the set-up in real conditions and to bring first results concerning on-line testings of memories.

## REFERENCES

---

- [1] “Radiation induced Edge Effects in Deep Submicron CMOS transistors”, Federico Faccio IEEE transactions in Nuclear Science December 2005
- [2] “A 0.13um CMOS Rad-hard proven technology with associated mixed mode circuit design approaches for space applications”, Laurent Dugoujon AMICSA 2006
- [3] “Unité de commande pour systèmes parallèles: contrôleur basé sur la mise en œuvre dynamique de réseaux de Pétri”, PhD thesis of Stéphane Chevobbe (2005) DTA/LIST/DTSI/SARC/06-07
- [4] “Microdosimètre EDF: compte-rendu d’essais du prototype industriel”, Alain Giraud, réf. DTA/LIST/DTSI/SARC/LCSD/03-164

## TASK LEADER

---

Alain GIRAUD

DRT/LIST/DTSI/SARC/LFSE  
CEA-Saclay  
F-91191 Gif-sur-Yvette Cedex

Tel. : 33 1 69 08 64 30  
Fax : 33 1 69 08 20 82

e-mail : alain.giraud@cea.fr

**UT-VIV/AM-HYDRO**

**Task Title: TECHNOLOGIES AND CONTROL FOR REMOTE HANDLING SYSTEMS**

**INTRODUCTION**

CEA in collaboration with CYBERNETIX and IFREMER has developed the advanced hydraulic robot MAESTRO. Thanks to control laws developed in the TAO 2000 controller, the MAESTRO can be used in a force reflective master-slave configuration.

Development around the actuating technology of the MAESTRO's hydraulic arm successfully proved on servovalves prototypes the interest to use pressure control servovalve instead of flow control servo-valve. The control is directly made on the pressure, i.e. the force which makes real improvement during force control modes which are extensively used in remote handling techniques.

In-LHC (French servo-valve manufacturer), developed a pressure servo-valve prototype that fits the MAESTRO's space constraints.

Operating in a fusion reactor requires a cleanliness level that oil hydraulics cannot ensure. Pure water hydraulics therefore proposes a good alternative and developments are today focusing in that direction. Feasibility of a pressure control valve running with water was proven and two prototypes were manufactured. Characterization of these prototypes was made on closed apertures. Although performances were not completely in agreement with the requirements, preliminary tests were run on a water hydraulic joint test rig.

**2006 ACTIVITIES**

**Servovalve's specifications**

Two prototypes were manufactured during year 2005 with the following requirements:

- Operating pressure 210bars
- Minimum flow rate 6 liters/min
- Bandwidth > 20Hz on half the volume of an "elbow axis" Maestro vane actuator
- Driving current +/- 10mA
- Leak rate minimum (aiming at < 1liter/min)
- Integrated dose rate 10kGy



Figure 1: Servovalve prototype

**Characterization of the servovalve**

A servovalve device consists in 4 subsystems (see figure 2):

- A torque motor (torque motor plus armature flapper)
- An hydraulic amplifier (flapper nozzle interface)
- A spool
- Two control ports

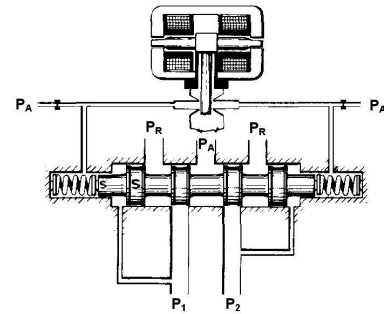


Figure 2: Principle of the pressure servovalve

From a macroscopic point of view equilibrium equations of the spool and the torque flapper-nozzle interface gives the following equations:

$$\Delta P = P_2 - P_1 = \frac{s}{S-s} (P' - P'') = \frac{s}{S-s} K.i = K'.i$$

Were K is the magnetic gain of the torque motor, i the current input and P' and P'' the two pilot pressures on both side of the spool (a bit lower than Pa, the supply pressure). Identification of these parameters are made on a test bench (see figure 3) to assess the performances of the prototype. Dead volumes can be connected to the bench to simulate the presence of an actuator.

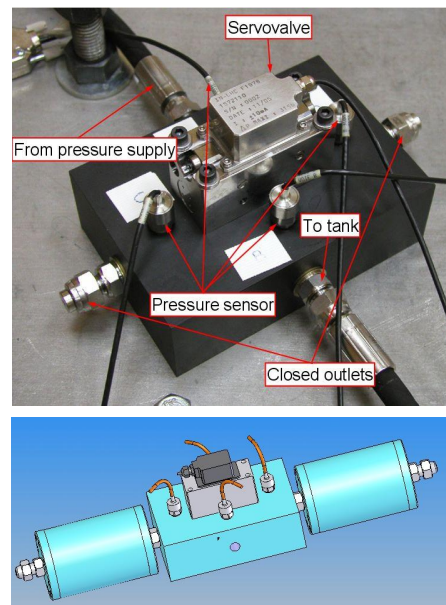


Figure 3: Test rig for water tests

Tests on closed apertures show some significant differences with the requirements. Although the control scheme could deal with the non linearity of the valve, full scale performances are 25% under the requirements and directly affect the available payload at the end of the arm (figure 4).

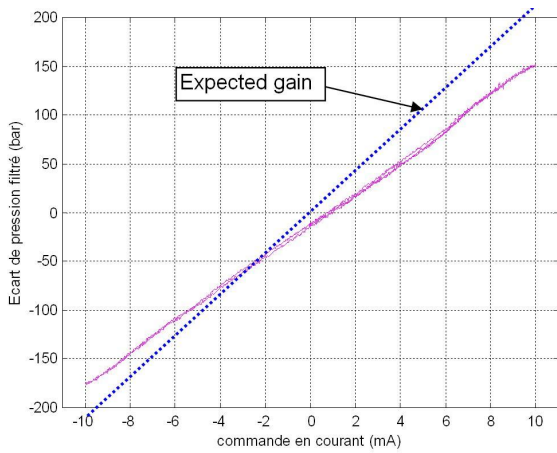


Figure 4: Measured and expected gain

Tests with presence of dead volumes show some significant effects on the dynamics of the servovalve (see figure 5). Both magnitude and phase of the servovalve are affected. One can also notice that modelling the servovalve with a classical second order equivalent model will not be accurate for high volumes.

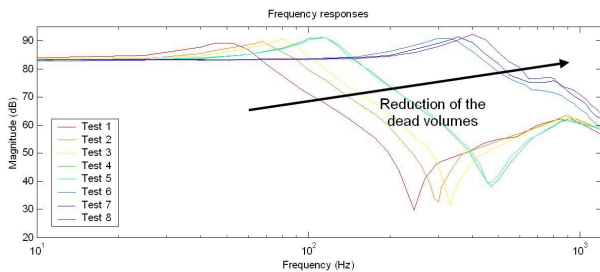


Figure 5: Effect of the presence of dead-volumes

### Characterization of the assembly servovalve + vane actuator

Although performances of the valve are below the expected requirements, its behavior was tested on the water hydraulic test bench (see figure 6).

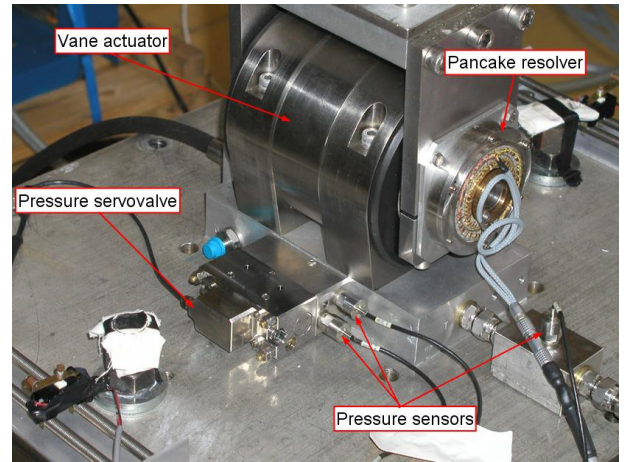


Figure 6: Water hydraulic test bed with pressure servovalve

Instabilities of the pressure servovalve were observed in case of sudden drop of input current (figure 7).

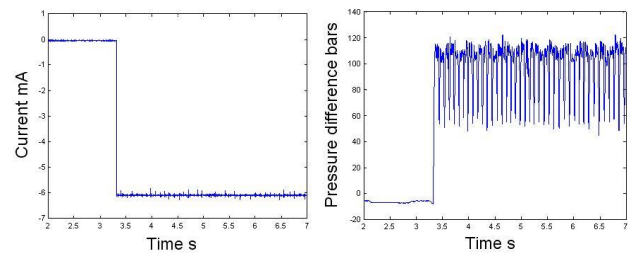


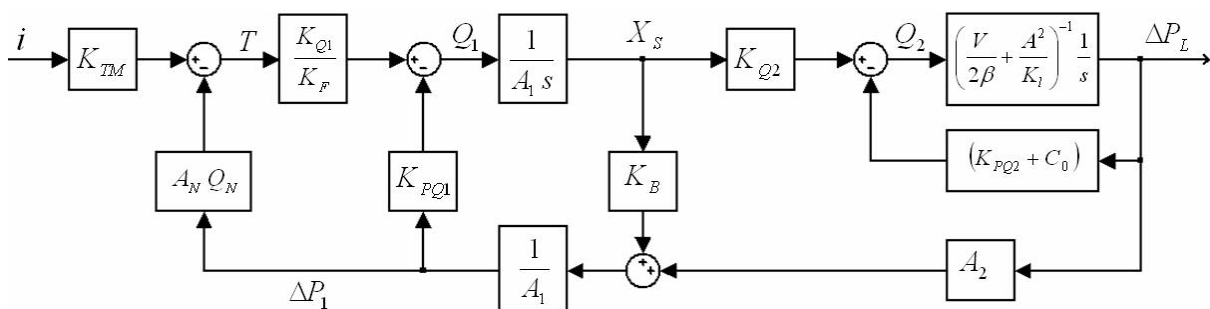
Figure 7: Pressure instability

Pressure instabilities and the 3000Hz noise associated to this phenomenon are generated by cavitation in the first stage of the valve. It seems possible to reduce this effect if the tank pressure is increased to 50bars and if a jitter signal is applied to the input current of the servovalve. For the present design, applying these solutions would mean another reduction of the gain. Solutions are under investigation to remove this effect.

### Servovalve model

In order to understand the behaviour of the servovalve and identify the effect of all parameters on the stability of the model, it is important to build a complete model of the valve.

First analysis concentrated on simplified block diagrams of the valve:



With:

Symbols	Significations	Units
$i$	Input current	mA
$T$	Torque on the armature/flapper	N.m
$Q1$	Hydraulic amplifier flow to the spool	L/min
$Q2$	Servo valve flow	L/min
$X_s$	Spool displacement	m
$\Delta P_1$	Hydraulic amplifier differential pressure	bar
$\Delta P_L$	Load differential pressure	bar
$K_{TM}$	Torque motor gain	N.m/mA
$K_{Q1}$	Hydraulic amplifier flow gain	L/(min.rad)
$K_{Q2}$	Spool flow gain	L/(min.m)
$K_{PQ1}$	Hydraulic amplifier loading effect	L/(min.bar)
$K_{PQ2}$	Spool orifice loading	L/(min.bar)
$K_B$	Spool Bernoulli force gradient	N/m
$K_F$	Net stiffness of armature / flapper	N.m/rad
$A_1$	Spool driving area	m <sup>2</sup>
$A_2$	Spool feedback end area	m <sup>2</sup>
$A_N$	Nozzle frontal area	m <sup>2</sup>
$Q_N$	Moment arm to nozzles	m
$\beta$	Fluid bulk modulus	bar
$V$	Load fluid volume (each side)	m <sup>3</sup>
$K_L$	Mechanical stiffness of load	N/m
$A$	Load drive piston area	m <sup>2</sup>
$C_0$	Bypass orifice flow	L/(min.bar)
$s$	Laplace operator	s <sup>-1</sup>

Although such a model helps to understand interactions between all elements of the servovalve evaluation or measurements of all the parameters of this model are difficult or impossible. To understand the behaviour of the servovalve, an advanced model using the intrinsic properties of the material is necessary.

Dynamic differential equations are written for each subsystem: torque motor + armature flapper, hydraulic amplifier, spool equilibrium, flow rate in the spool chambers, leading to the following eight non-linear equations.

These non linear equations are solved using physical block diagrams in Matlab-Simulink (see figure 8):

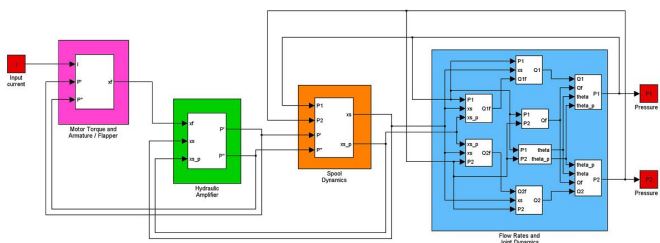


Figure 8: Advanced model block diagram

Adjustment of all parameters of the model allows building an accurate model and identifying the parameters having most importance on the equipment.

## CONCLUSIONS

Pressure control water servovalve prototypes were both tested with closed apertures and on dead volumes for qualification and characterization with water.

Performances of the existing prototypes do not reach the expected requirements. The change of fluid induced new physical phenomenon (cavitation) when the equipment is used in configuration similar to robotic applications. Modifications of the design of the valve are therefore necessary and under investigation to minimize the internal leaks and limit the cavitation effects.

Identifications of all parameters affecting the stability of the valve are under study in an advanced model of the servovalve.

## REPORTS AND PUBLICATIONS

CEA/DTSI/SRI/LTC/06RT020 Dynamic modelization and identification of a water-hydraulics pressure servovalve.

## TASK LEADER

Jean Pierre FRICONNEAU

DRT/DTSI/SRSI  
CEA-Fontenay aux Roses  
Boite Postale 6  
F-92265 Fontenay aux Roses Cedex

Tel. : 33 1 46 54 89 66  
Fax : 33 1 46 54 75 80

e-mail : jean-pierre.friconneau@cea.fr